Sequestration of Blood Plasma Iron as a Marker of Systemic Response to the Blast Lung Injury

Assessment with Electron Paramagnetic Resonance (EPR) Spectroscopy

Nikolai V Gorbunov
Walter Reed Army Institute of Research/MCR
Department of Polytrauma and Resuscitative Research
503 Robert Grant Avenue, # 1A14
Silver Spring, MD, 20910-7500
Tel (301) 319-9885
nikolai.gorbounov@na.amedd.army.mil

Stephen J McFaul
Walter Reed Army Institute of Research /MCR
Department of Blood Research
503 Robert Grant Ave.,
Silver Spring, MD, USA, 20910

Adolph Januszkiewicz
Walter Reed Army Institute of Research /MCR
Department of Polytrauma and Resuscitative Research
503 Robert Grant Ave.,
Silver Spring, MD, USA, 20910

COL James L Atkins
Walter Reed Army Institute of Research /MCR
503 Robert Grant Ave.,
Silver Spring, MD, USA, 20910

SUMMARY

Impact of blast shock waves (SW) with the body wall produces blast lung injuries characterized by bilateral traumatic hemorrhages. Such injuries often have no external signs, are difficult to diagnose, and therefore, are frequently underestimated. Predictive assessment of acute respiratory distress syndrome outcome in SW-related accidents should be based on experimental data from appropriate animal models. Blood plasma transferrin is a major carrier of blood iron essential for proliferative "emergency" response of hematopoietic and immune systems as well as injured tissue in major trauma. Iron-transferrin complexes ([Fe^{3+}]TRF) can be quantitatively analyzed in blood and tissue samples with low-temperature EPR techniques. We hypothesized that use of EPR techniques in combination with assays for pro-inflammatory cytokines and granulocytes in the peripheral blood and BAL would reveal a pattern of systemic sequestration of [Fe^{3+}]TRF that could be useful for development of biomarkers of the systemic inflammatory response to lung injury. With this goal we (i) analyzed time-dependent dynamics of [Fe^{3+}]TRF in the peripheral blood of rats after impacts of SW generated in a laboratory shock-tube and (ii) assayed the fluctuation of granulocyte (PMN) counts and expression of CD11b adhesion molecules on the surface of PMNs during the first 24 h after SW-induced injury. Sham-treated

Paper presented at the RTO HFM Symposium on "Combat Casualty Care in Ground Based Tactical Situations: Trauma Technology and Emergency Medical Procedures", held in St. Pete Beach, USA, 16-18 August 2004, and published in RTO-MP-HFM-109.

animals were used as control. Exposure to led to a significant decrease in the amount of blood [Fe^{3+}]TRF that correlated with the extent of lung injury and developed gradually during the first 24 h. Thus, sequestration of [Fe^{3+}]TRF occurred as early as 3 h post-exposure. At that time, the steady state concentration of [Fe^{3+}]TRF in blood samples decreased from 19.7±0.6 μM in controls to 7.5±1.3 μM in exposed animals. The levels of [Fe^{3+}]TRF remained decreased thoughout the entire study period. PMN counts increased 5-fold and 3.5-fold over controls respectively, at 3 and 6 h postexposure. These effects were accompanied by an increase in expression of CD11b on the surface membrane of PMNs. Extensive release of cytokines IL-1, IL-6, MCP-1, and MIP-2 was observed in BAL fluid and blood plasma during 24 h postexposure. We conclude that EPR monitoring of blood [Fe^{3+}]TRF can be a useful approach for assessment of systemic pro-inflammatory alterations due to SW-induced lung injury.

1.0 INTRODUCTION

Detonation of explosives generates blast shock waves (SW) which are usually characterized by of (i) amplitude of blast overpressure, (ii) frequency of sound, and (iii) kinetic energy of striking force, and are considered to be major factors that produce the blast-injured casualty [1 - 4]. A pattern of striking injuries ranges from displacement and rupture of bone and organs to amputations of limbs and can be assessed by the existing biomechanical models for high-velocity, low-mass impacts [1, 5, 6]. The effects produced by SW-generated sound and SW-generated overpressure are more complex and remain beyond the framework of predictive biomechanical models. These damaging effects often have no external signs, can be painless, difficult to diagnose and prediction of outcomes, are frequently underestimated, and therefore, need to be assessed at cellular and molecular levels [7-9].

Interaction of SW with the body wall or body armor produces two types of energy waves, high frequency {0.5 to 1.5 kiloHertz (kHz)} low-amplitude stress waves, and long duration {2 – 3 msec)} low frequency (below 0.5 kHz) share waves; both types of energy waves can be transmitted directly though tissues [3, 4, 10]. Stress waves move faster than the velocity of sound in tissue. Like ultrasound, they deposit energy wherever they are reflected or change their frequency, resulting in biomembrane fragmentations, edema, and hemorrhage [3, 4]. Therefore, lung, which contains many air/fluid interfaces where density changes abruptly, is particularly susceptible to stress wave injury [3, 4].

Share waves produce gross thoracic deformation in association with compression, distortion and stretching of alveolar walls. In this case, internal hemorrhage and pulmonary contusion are due to hyperbaric effects when stretching of alveolar capillaries overcomes their natural elasticity and barotrauma-like injury takes place [3, 4, 11]. Thus, it has been suggested that the criterion for injury due to blast-induced waves of high frequency is overpressure impulse, while overpressure per se is the determining factor if the wave frequency is low [12].

Multiple patho-physiological observations in animal models and clinics suggest that the major primary features of the SW-induced lung blunt trauma are pulmonary contusion, hemorrhagic lesions, edema, and circulatory depression [4, 13, 14]. The extravasated blood may be responsible for initiating a cascade of systemic reactions that involve expression and release of various vasoactive and pro-inflammatory humoral factors and vascular components. These presumably can activate inflammatory leukocytes for migration from the peripheral blood into the injured areas, where release of proteolytic enzymes and oxygen-derived free radicals aggravate parenchymal injury. Indeed, it has been documented recently that blast-induced blunt trauma is often complicated by secondary (indirect) acute lung injury (ALI) and acute respiratory distress syndrome (ARDS), apparently due to infiltration of neutrophils (PMNs) [15].

Among the essential biochemical changes related to the inflammatory response to trauma is the increased turnover of serum concentrations of transferrin-chelated iron ([Fe^{3+}]TRF), which represents the main pool of blood plasma iron [16 – 18]. The levels of plasma iron ([Fe^{3+}]) fall as a result of iron redistribution from plasma to tissues [16]. The trauma-induced iron sequestration (hypoferremia) has been observed in the

pathogenesis of trauma of different etiology and has been documented in blast lung injuries of different severity [19, 20].

The objective of the present research was to evaluate [Fe^{3+}]TRF status in the peripheral blood of rats during an inflammatory response following exposure to medium amplitude {(~90 or ~120 kiloPascals (kPa)} low-frequency 260±5 Hertz (Hz) SW, as a biomarker of severity of lung injury.

Each experiment included a pathology assessment using an injury scoring system developed for blunt trauma injuries to derive a severity score for lung damage [21]. Inflammatory response was estimated from immunoassays for pro-inflammatory cytokines and assessments of alteration in inflammatory leukocytes in the peripheral blood and injured lung. Amounts of [Fe^{3+}]TRF in whole blood and blood plasma samples were measured by quantitative electron paramagnetic resonance (EPR) spectroscopy. The observed alterations in the amounts of blood [Fe^{3+}]TRF were correlated with estimated injury score (IS) ratios in each animal. The gathered data suggested that stress-induced tissue sequestration of [Fe^{3+}]TRF from the peripheral blood can be considered as a potential biomarker of the systemic inflammatory alterations due to blast lung trauma.

2.0 MATERIALS AND METHODS

2.1 Treatment of Animals

CVF Sprague-Dawley rats, weight 280-320 g, were purchased from Charles Rivers Laboratories Inc., Wilmington, MA. The rats were acclimatized for 7 days during which they were maintained in a unidirectional filtered-air room with 12/12 h light/dark cycle and allowed food and water *ad libitum*. Following acclimatization, rats were randomly assigned to the "SW exposure" and "control" groups. Then, all animals were anesthetized with ketamine + xylazine (60 mg + 5 mg per kg of body weight, IP), and animals from the "exposure" group were subjected to lung trauma by impact of SW. The compressed air-driven shock tube generated a single SW with main harmonic frequency at 260±5 Hz and peak overpressure at 90±5 kPa or 122 ± 8 kPa (at peak overpressure, see Fig. 1). The pressure-time history of SW was recorded at each exposure. This study focused on the effects at different time periods and used a sequential approach to post-exposure events. Phase I of the study design called for analysis of pro-inflammatory alterations and alterations in [Fe^{3+}]TRF at 1, 3, 6, 12, and 24 h following exposure to SW with main harmonic frequency at 260±5 Hz and peak overpressure at 122 ± 8 kPa. Previous experiments demonstrated that at this level of overpressure produced the most consistent lung injury [22]. Accidents of lethal outcome (mortality rate was ~25%) usually developed during the first 15 min of post-exposure and were excluded from further analyses. Thus, the 32 rats that survived were subjected to blood and lung tissue sampling at 1, 3, 6, 12, and 24 h following exposure. Eighteen control animals underwent all procedures (i.e. anesthesia, suspension, time delays, etc.), except exposure.

Phase II was implemented in order to assess alterations in the amounts of TRF-[Fe3+] in the peripheral blood at 24 h following exposure to SW of either 90±5 kPa (7 animals**)** or 122±8 kPa (7 animals**)** to determine overpressure-dependent responses of the above parameter. Five sham-treated animals underwent all procedures (i.e. anesthesia, suspension, time delays, etc.), except exposure to SW.

Blood was drawn by cardiac puncture. Each individual animal was assigned only one sampling procedure. Blood samples for EPR, flow cytometry, and ELISA analyses were collected separately in 1 cc and 3 cc syringes. Gross lesions were recorded and photographed. To avoid possible re-distribution of the infiltrated cells, the histology assessment was conducted in non-perfused lung.

Animal handling and treatments were conducted in compliance with the Animal Welfare Act and other Federal statutes and regulations related to animals and experiments involving animals adheres to principles stated in the Guide to the Care and Use of Laboratory Animals, National Research Council. The facilities are fully accredited by the Association for Assessment and Accreditation of Laboratory Animal Care International.

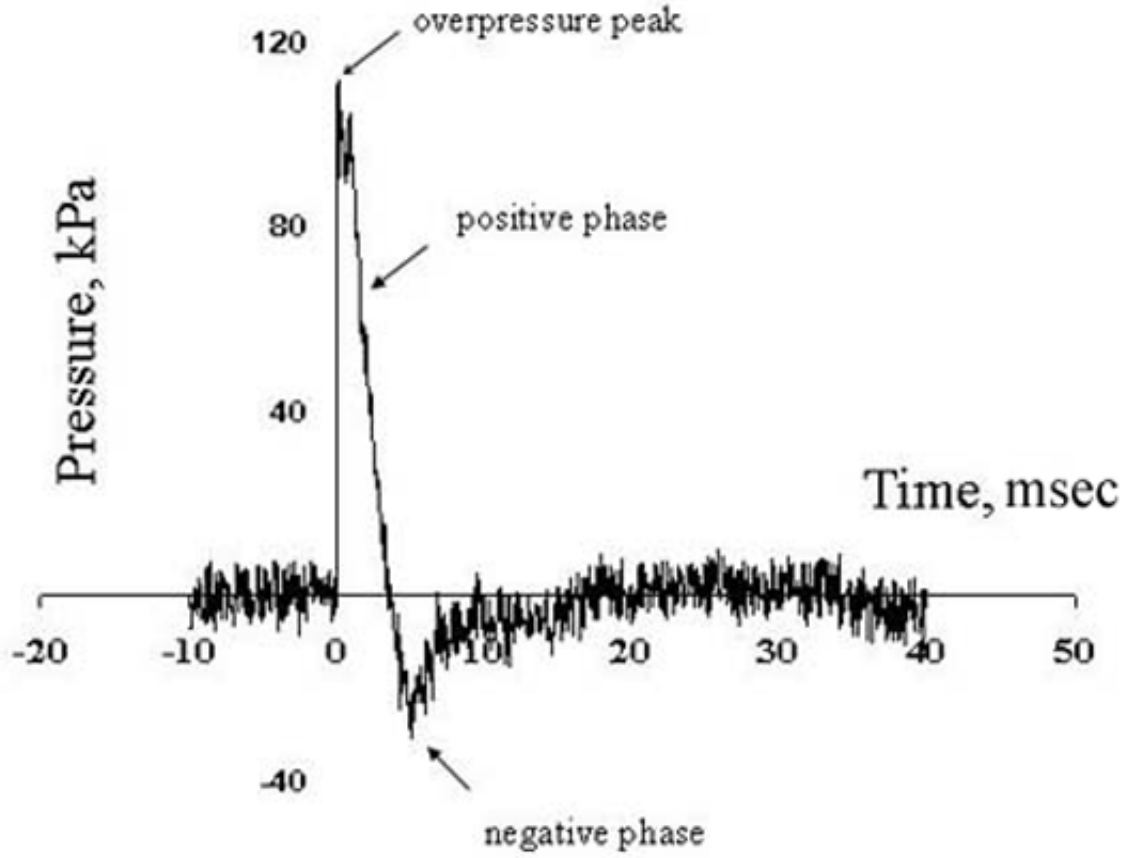

Figure 1. A graph illustrating the pressure-time history of a real SW with arrowed peak overpressure. Positive and negative phases of SW are arrowed. Peak overpressure has been defined as maximum pressure at the positive phase of SW.

2.2 EPR Analysis

Assessment of blood [Fe^{3+}]TRF was conducted with low-temperature EPR spectroscopy as described previously [20]. Briefly, 0.6 ml of blood was collected in 1 cc syringes free from latex and silicone oil (Henke-Sass, Wolf; Gmbh, Germany) to make blood samples of constant volume and geometrical profile. The drawn blood samples were frozen immediately in liquid nitrogen. The frozen samples were kept at -196 ^{O}C until EPR analysis was completed. Concentrations of blood [Fe^{3+}]TRF were calculated using standard solutions of apo-transferrin loaded with known amounts of [Fe^{3+}]. To prepare standard solutions of iron ([Fe^{3+}]) complexes with apo-TRF, i.e. [Fe^{3+}]TRF, a 0.1 mM solution of commercial human apo-TRF (M.W. ~80 kDa) (Sigma-Aldrich Chemical Co., St. Louis, MO) in Hanks' balanced salt solution (HBSS) (Life Technologies, Gaithersburg, MD) was titrated with 1.0 mM complex of [Fe^{3+}] with nitrilotriacetic acid {[Fe^{3+}]NTA_2 } in 0.5 M sodium bicarbonate buffered solution, pH 7.2, for 10 min. [Fe^{3+}]NTA_2 was prepared by incubation of nitrilotriacetic acid (N,N-bis[carboxymethyl]glycine) trisodium salt (Sigma-Aldrich Chemical Co., St. Louis, MO) with ferric chloride (Fisher Scientific, Fair Lawn, NJ) in 0.5 M sodium bicarbonate (Fisher Scientific, Fair Lawn, NJ) buffered solution, pH 7.2, for 10 min at room temperature. The frozen samples of [Fe^{3+}]TRF solutions were kept at -196 ^{O}C during the EPR experiments. The characteristic profile of the recorded low temperature EPR spectra of [Fe^{3+}]TRF standard solutions were compared to the spectrum of 0.1 mM solution of holo-transferrin (Sigma-Aldrich Chemical Co., St. Louis, MO) in Hanks' Balanced Salt Solution (pH 7.4). The recorded EPR spectra were integrated using the WINEPR program package (Bruker, Co). The second integral values were used to calculate concentrations of [Fe^{3+}]TRF in blood samples.

2.3 Flow Cytometry

For flow cytometry analysis of CD11b in PMNs, blood was drawn into syringes that contained 50 USP U heparin/ml (SoloPark Laboratories, Franklin Park, IL, 60131). The samples on a given day from the exposed and control animals were processed in parallel. The 1cc syringes that contained heparinized blood samples were kept on ice at 0° C until the cells were labeled with monoclonal antibodies. Cell labeling for flow cytometry was conducted as follows: aliquots (100 µl) of the heparinized blood were transferred into sterile polypropylene tubes and labeled either with 5 µg/ml of mouse anti-rat CD11b-biotin antibody, (IgA), (BD PharMingen, San Diego, CA) or 5 µg/ml of mouse IgA isotype-biotin antibody, (BD PharMingen, San Diego, CA) for 20 min at room temperature. Then, 2 ml of 1x BD Facs Lyse Solution (BD Bioscience, San Diego, CA) were added to each sample to lyse the erythocytes. After 10 min, the leukocytes were centrifuged at 2,000 x g for 5 min, washed twice with Tyrode's buffer, resuspended in 0.1 ml of Tyrode's buffer, and incubated with 20 µl of streptavidin-PE (17 µg/ml) (BD PharMingen, San Diego, CA) for 20 min. Then 500 µl of Tyrode's buffer were added and the cells were assessed by flow cytometry. Unlabeled control cells were treated as above, except, they were not labeled with CD11b-biotin antibody nor incubated with streptavidin-PE.

A Becton-Dickinson FACSort flow cytometer and CELLQuest Pro software (Becton Dickinson) were used for acquisition and analysis of the data. PMNs were identified by their side- and forward light scatter coupled with fluorescence in the FL2 channel due to CD11b-specific fluorescence labeling with antibody conjugated to phycoerythin (PE). The CD11b expression on PMNs was evaluated by creating FL2 (CD11b) histograms and gating on FL2 positive cells in the FL2 *vs*. SSC dot plot. Positive CD11b specific immunofluorescence of PMNs was distinguished from the isotype immunofluorescence (negative control for nonspecific immunoadherence) in all samples. CD11b expression was proportional to the mean fluorescence intensity (MFI) in the FL2 channel and is presented in relative fluorescence units. The PMN numbers in blood samples are presented as PMN counts per 10000 events.

2.4 Analysis of MIP-2 in Blood Plasma Samples

For enzyme-linked immunosorbent assay (ELISA) analysis of rat MIP-2, 3 ml of blood were drawn into a solution of ethylenediaminetetracetic acid disodium salt (EDTA) (1mg/ml in 0.1 M PBS pH 7.4). Cells were removed by centrifugation (2,000 x g for 5 min). The blood plasma samples that exhibited signs of hemolysis were excluded from further analysis. Blood plasma was aliquoted into 1.5 ml polypropylene vials and stored at –80 ^{O}C until analyzed. Concentrations of blood plasma MIP-2 were quantified with an immunoassay kit from BioSource International Inc. (Camarillo, CA) according to the manufacturer's protocol.

2.5 Cytokine Analysis in BAL Fluid

BAL fluid samples were obtained though the trachea after incision in the neck following euthanasia. The lungs were lavaged with 3 ml volume of Dulbecco's Phosphate Buffered Saline (pH 7.4) though a cannula inserted into the trachea. Cell pellets were pooled from the lavages and centrifuged at 1,200 *g* for 10 min. The supernatants were collected and frozen immediately in liquid nitrogen, and stored at –80^{o} C until analyzed for IL-1b, IL-6, INF-g, and MCP-1 cytokines using LINCOplex Rat Cytokine/chemokine Kit and the Luminex® 100 IS System (LINCO Research, Inc., St. Charies, MO, www.lincoresearch.com).

2.6 Evaluation of Blunt Trauma Injury

Injury score (IS) for -induced pulmonary trauma in rats was assessed using an injury scoring system developed recently for air blast-induced blunt trauma [21]. Briefly, the scoring system utilized a packet of scoring sheets to aid in assessment of lesions [21]. Each sheet was designed to provide a quantitative assessment of the severity of the lesions in lung as defined by the equation:

$$IS = (E+G+ST)(SD)$$

where E, G, ST, and SD were defined as:
E, extent of injury in terms of lung lobes, (0-5 range); G, injury grade, which included the extent of surface area of the lesions, (0-4 range); ST, severity type element that classifies the type of the worst-case lesions (i.e. petechiae, punctures, ruptures), (0-5 range); SD, severity depth element which indicates the depth of disruption of the worst-case lesion, (1-4 range). The Severity of Injury Index (SII) was then calculated as: IS/Maximum Possible IS for rat lung, i.e."56". Thus, the assigned lung SII was 0.0 for "negative injury level," 0.03 though 0.04 for "trace injury level," 0.05 though 0.21 for "slight injury level," 0.22 though 0.36 for "moderate injury level" and 0.37 though 0.64 for "extensive injury level." At the selected experimental conditions the estimated SII levels ranged from 0.22 though 0.36 and, therefore, were characterized as "moderate injury levels" [21].

2.7 Lung Tissue Preparation for Histology and Immunofluorescence Microscopy

Lung tissue samples were collected at necropsy, fixed in 4% buffered paraformaldehyde (pH 7.4), embedded and frozen in O.C.T. compound, and subjected to cryosectioning. The obtained specimens (10 μm sections) were stained with hematoxylin and eosin for histological examinations or processed for immunofluorescence analysis with light, or fluorescence confocal microscopy respectively.

2.8 Immunofluorescence Techniques and Image Analysis

The obtained lung specimens (see above) were processed for the immunofluorescence imaging as described previously (*23*). Briefly, the tissue sections were washed with phosphate buffered saline (PBS), incubated in PBS containing 2% paraformaldehyde and 0.1 % Triton X-100 for 20 min, washed thee times with PBS, then once with PBS containing 0.5% BSA and 0.15% glycine (buffer A). Any non-specific binding was blocked by incubating the samples with donkey normal serum (Santa Cruz Biotechnology, Inc., Santa Cruz, CA, www.scbt.com) diluted 1:20 in buffer A. The primary antibody against (I) VE-cadherin (goat polyclonal IgG from Santa Cruz Biotechnology, Inc., Santa Cruz, CA, www.scbt.com) and (II) MPO (rabbit polyclonal IgG from Calbiochem, San Diego, CA, www.calbiochem.com) were used in 1:250 dilution in buffer A. This was followed by thee additional washes with buffer A and incubation with secondary fluorochome-conjugated antibody, and with Heochest 33342 (Molecular Probes, Inc., Eugene OR, www.probes.com) diluted 1:5000. The labeled specimens were rinsed, mounted in Gelvatol (Monsanto Corp., St. Louis MO), and coverslipped for fluorescence microscopy. The specimens were analyzed with Nikon Eclipse E800 microscope (Nikon Plan Apo 60xA/1.4 lens) equipped with Bio-Rad 2100 confocal system. Image processing and analysis were conducted using C-Imaging software (Compix Inc., Cranberry Township PA).

2.9 Statistical Analysis

Tables of summary statistics and graphical displays were constructed to contrast the effects of primary outcomes variables. Analysis of variance procedures with Tukey post hoc correction examined the existence and nature of temporal trends among the treatment (viz., sampling time periods post exposure) level means. Significance is reported as $p<0.05$

3.0 RESULTS

3.1 Lung Injury Analyses: Pathology Scoring and Histology

It is well documented that impact of SW is associated with so called “primary injuries” that are largely restricted to the air-filled organs (e.g. lung, ears) [4, 14, 15]. The most consistent lung lesions that occurred after exposure to at peak overpressure of 122 ± 8 kPa, were bilateral diffuse parenchymal hemorrhages that involved the entire thickness of lobes as shown in Fig. 2B (compare to control, Fig. 2A).

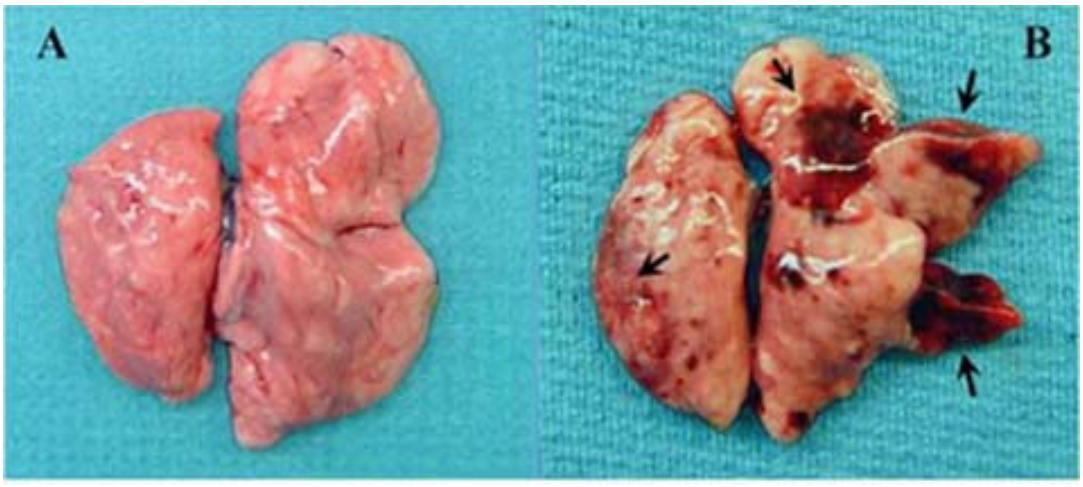

Figure 2. Representative macroscopic views of lung harvested from a control rat (A) and rats subjected to "moderate" (B) injury at 24 h after exposure to SW at peak overpressure of 118 kPa. Arrows in panel "B" show hemorrhagic lesions.

Pulmonary contusions were often accompanied by apnea that lasted up to 10 min following exposure. Histopathologic examination revealed significant hemorrhage of alveolar septal capillaries (Fig. 3). Pulmonary infiltration of PMNs and attachment of PMNs to erythocyte conglomerates was readily observed at 3, 6, 12, and 24 h (Figs. 3 C, D, E, F) but not at 1 h, (Fig. 3 B).

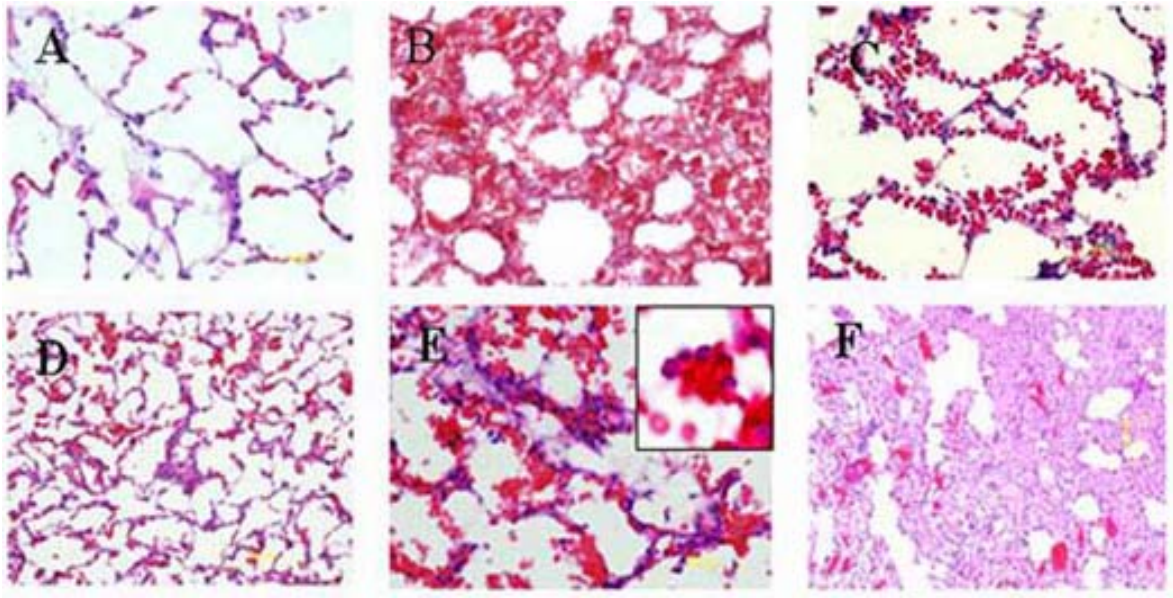

Figure 3. Representative histological sections of lung harvested from a sham-treated rat (A) and rats subjected to "moderate" injury at 1 h (B), 3 h (C), 6 h (D), 12 h (E), and 24 h (F) following SW exposure. Note, infiltrated PMNs attached to erythocyte conglomerates, observed at 12 h and 24 h.

All sections were stained with hematoxylin and eosin as described under "Materials and Methods". Images were digitally captured at 40x magnification (for "A", "B", "C", and "E"), and at 20x and 10x magnification (respectively for "D" and "F") to demonstrate the extent of PMN infiltration. Inset was captured at 100x magnification to demonstrate interaction of PMNs with extravascular erythocytes (in "E").

Immunofluorescence imaging of hemorrhagic lesions revealed that endothelial sequestration and transmigration of granulocytes observed at 3 though 24 h postexposure was accompanied by an appearance of immunoreactivity of myeloperoxidase in alveolar wall (Fig. 4).

Several lines of evidence suggest that early effector cells in the pathogenesis of trauma-induced ARDS are the PMNs that have demarginated from vascular endothelium and/or have been released from bone marrow, and, then infiltrated and deposited in lung [24, 25]. PMN-mediated tissue injury does not occur unless PMNs, primed and attracted by chemokines, migrate into surrounding parenchyma [24, 25, 26]. Therefore, in the next set of experiments we analyzed levels of chemokine MIP-2 in blood and induction of CD11b in PMNs at different post-exposure time-points using ELISA and immunofluorescence techniques, respectively.

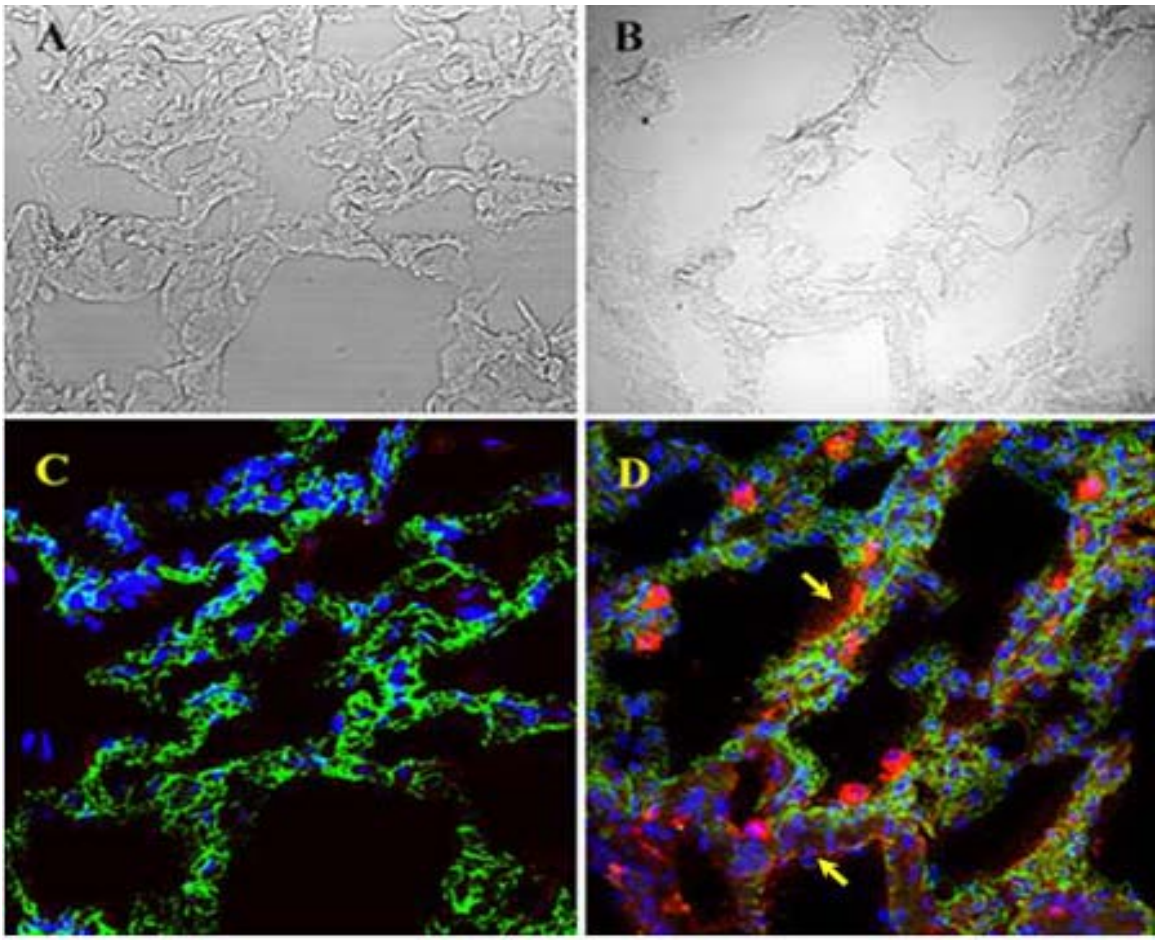

Figure. 4. Representative immunofluorescence images of lung specimens from sham-treated rat and rat subjected to "moderate" injury at 3 h following SW exposure. Assessment of infiltration of inflammatory leukocytes into alveolar septa was conducted with immunostaining for myeloperoxidase (MPO) and vascular endothelial marker - cadherin (VE-Cadherin).
Panels "A" and "B" bright field images of specimens from sham-treated and SW-exposed animals respectively. Panels "C" and "D" immunofluorescence images of mapping of VE-cadherin (green, Alexa 488) and MPO-abundant leukocytes (red, Cy3) in sham-treated and SW-exposed animals respectively. An appearance of the MPO immunoreactivity in alveolar septa in hemorrhagic lesions due to degranulation of leukocytes is arrowed in the panel "D".
Note: sections of hemorrhagic lesions of SW-exposed lung were used for preparation of the specimens as described in *Materials and Methods*. Confocal digital images were taken using Nikon Plan Apo 60xA/1.40 lens.

3.2 Cytokine/Chemokine Analysis of Blood Plasma and BAL Fluid

The rat chemokine MIP-2 (equivalent to human IL-8) is highly PMN-selective and, therefore, can be useful to predict early inflammatory phases of ARDS. Alteration in MIP-2 status was monitored in the peripheral blood of injured animals. Levels of MIP-2 in plasma were elevated at 1, 3, and 6 h following injury. Plasma MIP-2 increased from 2.9±2.6 pg/mL in control rats, to 33.0±7.9 pg/mL, 35.0±7. 3 pg/mL and 78.9±20.5 pg/mL at 1 h, 3 h, and 6 h respectively, in injured rats.

Alterations in the chemokine/cytokines in BAL are shown in Fig. 5. A substantial increase in the levels at 24 h post-exposure occurred within MCP-1 that apparently associated with the extensive phagocyte activity at that time.

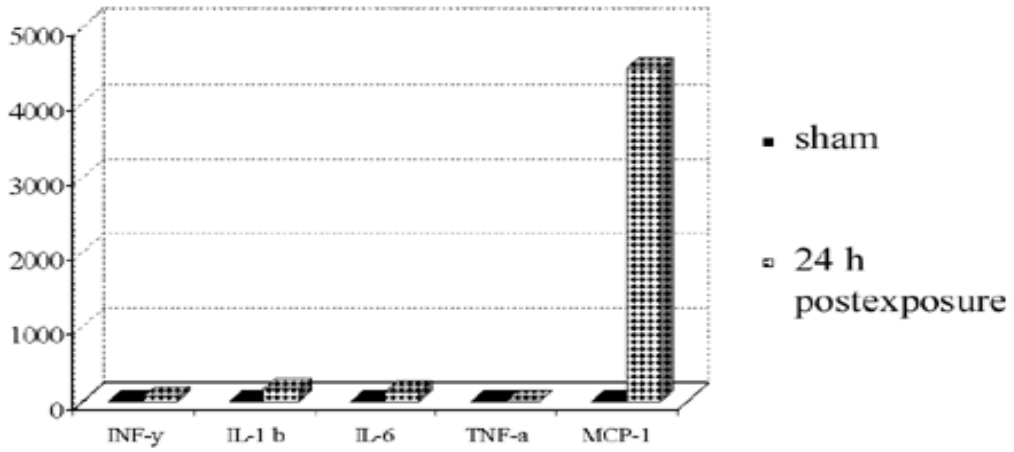

Figure. 5. Relative increase in the levels of inflammatory cytokines/chemokines in BAL fluid at 24 h following "moderate" lung injury. Collection of BAL fluid and the cytokines/chemokines assay were conducted as described in *Materials and Methods*.

3.3 Flow Cytometric Analysis of Blood PMNs

Fig. 6 shows that shock wave - induced moderate trauma was accompanied by rapid PMN recruitment and development of a neutrophilia at the first hour following exposure to shock wave as evidenced by increased PMN counts in blood samples. The number of PMNs in peripheral blood at this time increased from 1090±66 PMNs per 10000 events in the "control" group to 2948±359 PMNs per 10000 events in the "injury" group. PMNs in the blood of injured animals continued to increase at 3 h post-exposure to 5458±92 PMNs per 10000 events. A significant relative decrease of the above effect occurred during the later time-points of observation (i.e. 6, 12, and 24 h) (Fig. 6), which probably reflected PMN sequestration by target tissues. Still, the steady state counts of blood PMNs at 6, 12, and 24 h following exposure remained significantly above control counts, i.e. 3850±315 PMNs, 3351±293 PMNs, and 2400±442 PMNs per 10000 events.

The early (1 h) increase in the numbers of PMNs in the peripheral blood was not accompanied by a significant increase in expression of CD11b (Fig. 7). The observed increase in mean fluorescence intensity (MFI) for CD11b expression from 1928±51 A.U. to 2314±112 A.U. was not statistically significant. A significant augmentation of MFI was observed, however, at all time points from 3 h to 24 h following exposure (Fig. 7).

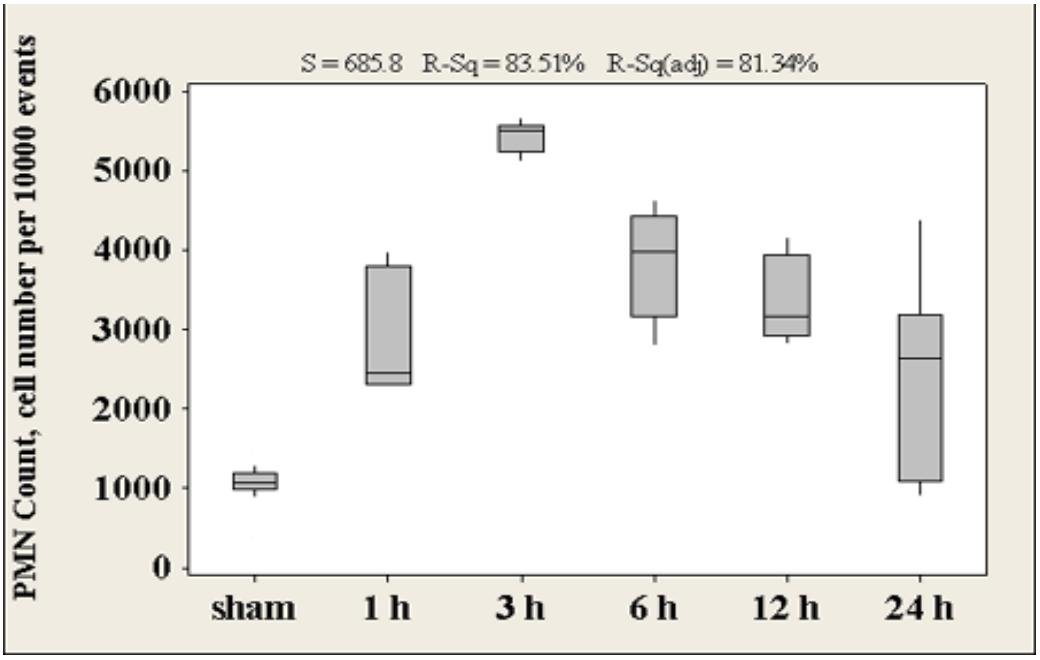

Figure. 6. Effect of SW exposure on PMN counts in rat peripheral blood at different time periods of blood sampling.
Values are least squares means for PMN counts in box plots ranging from the 25th to 75th percentile. Bars indicate the 5th and 95th percentiles.

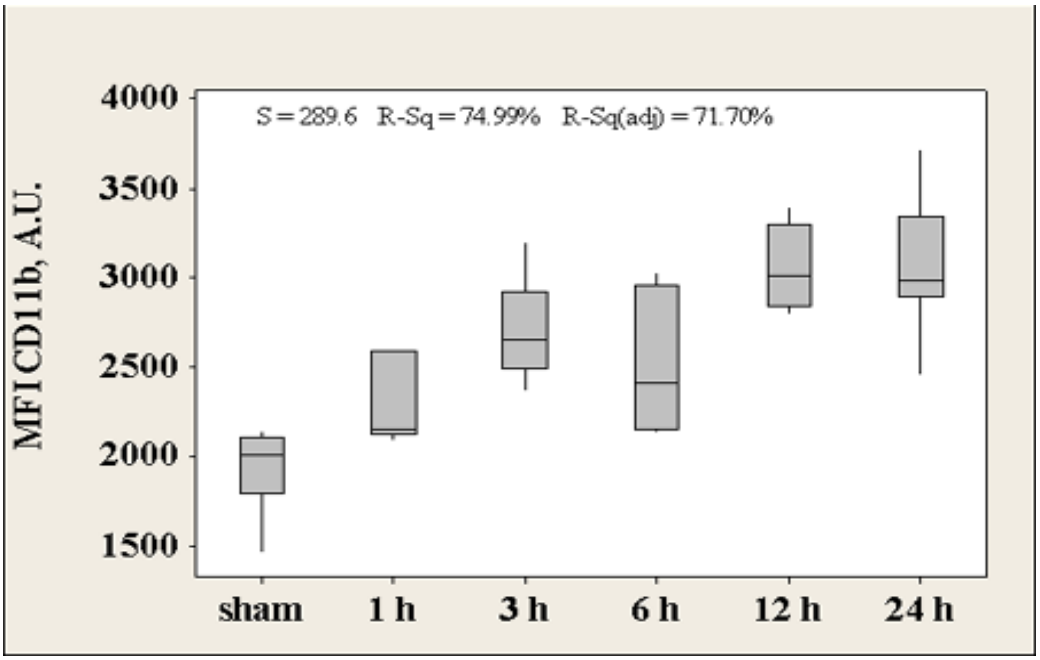

Figure. 7. Effect of SW exposure on CD11b expression in PMNs of rat peripheral blood at different time periods of blood sampling.
Values are least squares means for mean fluorescence intensity (MIF) in box plots ranging from the 25th to 75th percentile. Bars indicate the 5th and 95th percentiles.

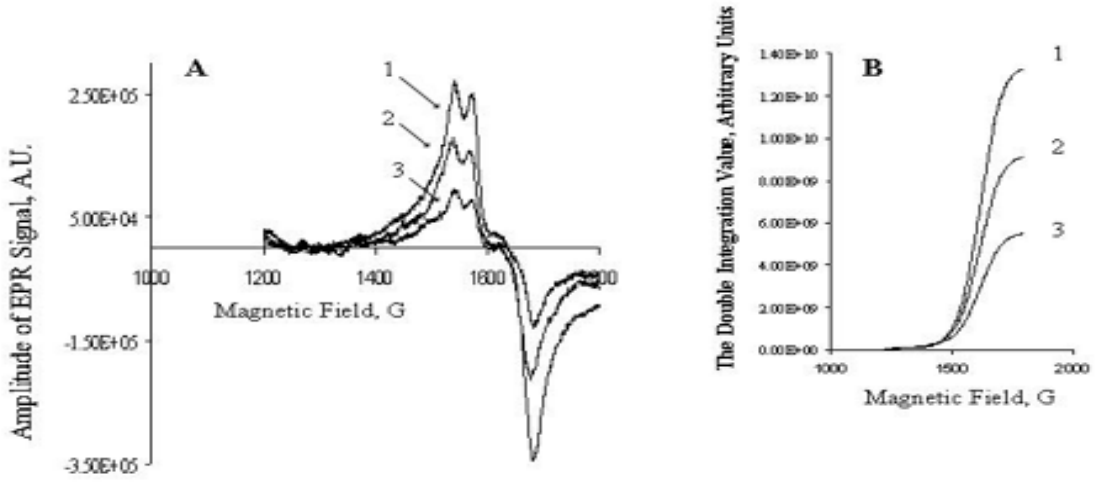

Figure 8. Representative low-temperature EPR spectra of transferrin-bound iron (TRF-[Fe^{3+}]) in rat blood at 24 h following SW exposure.

(A) - EPR spectra of blood TRF-[Fe^{3+}] and respective second integral curves (B) from "1" – sham-treated rat ("negative injury"), "2" - rat experienced "slight injury", "3" – rat after "moderate injury". Injury Levels were estimated as described in *Materials and Methods.*

3.4 Low Temperature EPR Analysis of Transferrin-Bound Iron in Rat Blood Samples

The quantitative conditions for the effect of resonance microwave energy absorption by electrons (i.e. EPR) can be given by:

$H = h\nu/\beta g$

where H = the resonance magnetic field, in Gauss (G),

(see spectra in *Results*)

h = Planck's constant (6.625×10^{-27} erg-sec)

ν = resonance microwave frequency (9.463 GHz),

from EPR spectrometer settings

β = the Boh magneton (constant)

g = factor of spectral splitting

Since the g factor values are constant for each type of paramagnetic center, the g factor can be considered as a quantity characteristic of the molecule in which the unpaired electrons are located. Low temperature EPR signals of paramagnetic [Fe^{3+}] (i.e. high spin d^5Fe^{3+}, S = 5/2) coordinated in the interdomain cleft of each of the lobes (C and N) of the transferrin molecule are identical due to the nature of the ligands in the [Fe3+] coordination sites. Note each of the two EPR signals from [Fe3+] chelated in the C-lobe and N-lobe additively contributes to the resulting EPR spectrum of the diferric transferrin molecule. The main component of this spectrum (at 77^{o} K) has a characteristic doublet maximum with major features at g = 4.30 and 4.40 (trough at g = 4.03) that belong to high spin d^5Fe^{3+} in a rhombic environment (symmetry) (Fig. 8 A). During computation of the concentration of [Fe^{3+}] chelated by blood transferrin, diferric transferrin was considered to contain twice the amount of spins than each of C- and N-monoferric transferrins.

In heterogeneous, non-light transparent systems such as blood, spin concentration values may be the only possible quantitative measurement, and may be useful when the molecular species are unidentified or chelated within labile complexes. For quantitative estimates of spin concentration, usually the computed second integral of the derivative curve (Fig. 8 B) is compared with that of a standard sample. The spin concentration in an unknown sample (N_x) is related to the number of spins in a standard sample (N_s) by the equation:

$N_x = k\, \Sigma_x/\Sigma_s\, N_s$

where sub s and x designate the standard and unknown samples, respectively; Σ, the integral of the EPR absorption over the entire EPR signal; and k, a constant that includes EPR spectrometer settings and sample

geometrical profile (geometry). Note sample geometry and EPR spectrometer settings were constant in the conducted experiments. The parameters Σ_x, and Σ_s were calculated from EPR spectra of blood, blood plasma samples, and standard solutions of [Fe^{3+}]TRF.

Representative low temperature EPR spectra of [Fe^{3+}]TRF in blood samples from rats with "negative," "slight" and "moderate" injuries are shown in Fig. 8 A, spectra 1, 2, and 3 respectively. The respective double integration values are shown in Fig. 8 B. As follows from the presented results, systemic response to SW-induced trauma in rat subjected to a "moderate" injury level was accompanied by ~60 % decrease in the amount of blood [Fe^{3+}]TRF, while "slight" injury caused ~30 % decrease of the same parameter in comparison with "negative" injury in "sham-treated" rat.

Based on the above observations we expected most consistent inflammatory alterations due to exposure to at peak overpressure of 122 ± 8 kPa, which produced "moderate" injury in rats. Fig. 9 shows that there were no significant alterations in the amounts of blood [Fe^{3+}]TRF at 1 h post-exposure, but significant [Fe^{3+}]TRF sequestration occurred at 3 h post-exposure. At that time, the steady state concentration of [Fe^{3+}]TRF in blood samples decreased from 19.9±2.3 μM in controls to 7.6±2.5 μM in exposed animals. The levels of [Fe^{3+}]TRF remained decreased though out the entire period of observations up to 24 h (Fig. 9).

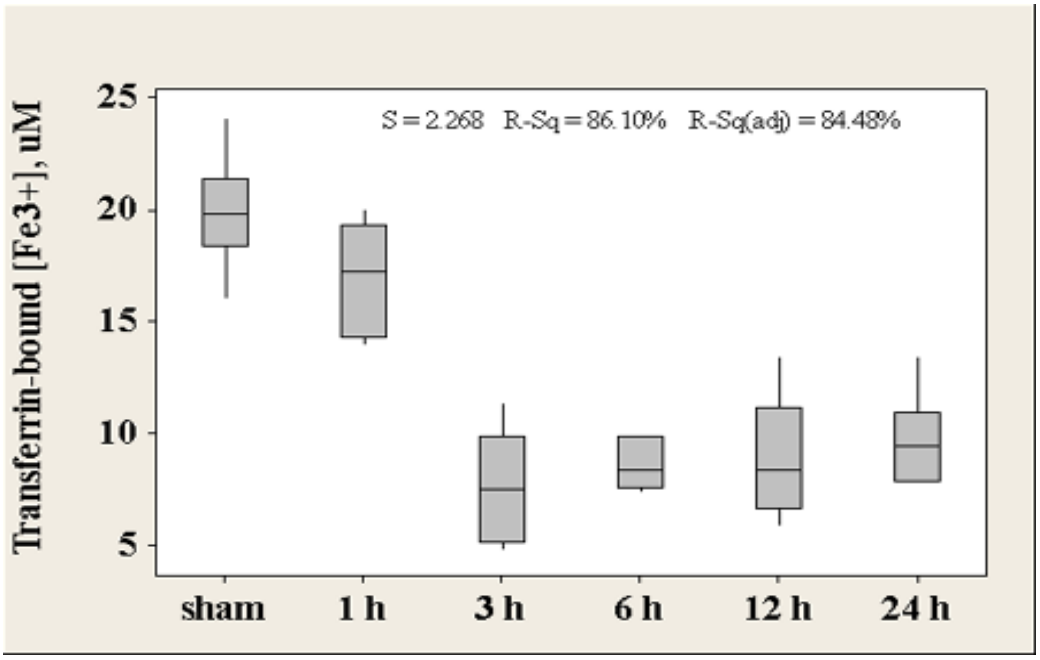

Figure. 9. Effect of SW exposure on the level of [Fe^{3+}]TRF in rat peripheral blood at different time periods of blood sampling.
Values are least squares means for concentration of [Fe^{3+}]TRF in box plots ranging from the 25th to 75th percentile. Bars indicate the 5th and 95th percentiles.

Regression analysis of the amounts of blood [Fe^{3+}]TRF on injury levels (i.e. "negative"- 0, "slight"- 2, and "moderate"- 3) showed significant inverse correlation between these two events (Pearson correlation of injury level and [Fe^{3+}]TRF r = -0.90) (Fig. 10). Indeed, the amount of [Fe^{3+}]TRF in blood dropped from 22.7±3.7 µM for the "negative" group to 15.2±1.4 µM in the "slight" injury group ($p<0.009$, n=7 Tukey test), and to 7.2±2.8 µM in the "moderate" injury group ($p<0.006$, n=7, Tukey test). Similar effect was observed in blood plasma. Thus, while the amount of [Fe^{3+}]TRF in blood plasma in the "negative" group was 31.0±1.8 µM, the same parameter in the "moderate" injury group was only 12.3±2.2 µM ($p<0.005$, n=7 Tukey test).

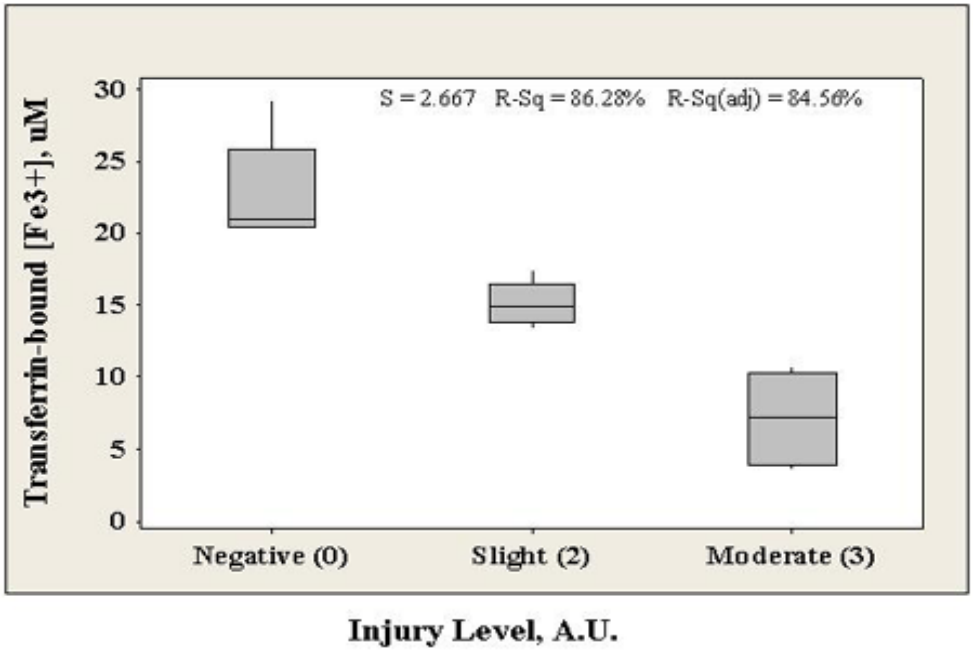

Figure 10. Regression plot of the amounts of transferrin-bound iron in blood samples on injury levels at 24 h following exposure to SW. Note, "negative injury" ("0") assigned to "sham-treatment". Values are least squares means for concentration of [Fe^{3+}]TRF in box plots ranging from the 25th to 75th percentile. Bars indicate the 5th and 95th percentiles.

4.0 DISCUSSION

Detonation of explosive materials or firing of large caliber guns generates a wide spectrum of shock waves in the ambient environment. Exposure to shock waves can cause serious internal injury mostly to air-filled organs like lung and bowel, without external indications of trauma [1-4].

Recent observations suggest that several different mechanisms are probably responsible for the various manifestations of blast-induced pulmonary insufficiency. Thus, while the immediate pulmonary injury are mostly characterized by apnea, barotraumatic air embolism, and internal bleeding, the delayed respiratory malfunctions that occur 24-48 h after blast accidents, are likely due to response to the damage to the tissue barriers and extravasation of blood components [4, 26, 27]. Indeed, respiratory failure that occurs 24-48 h after blast accidents was mostly associated with subsequent systemic inflammation [4, 28]. To date, most

human studies of systemic inflammation have focused on patients with clinical manifestation of pulmonary insufficiency and ARDS, and the sequence of inflammatory events that lead to these pathologies has not yet been clearly delineated [4, 28]. Furthermore, predictive diagnostics for the outcome of blast-induced trauma must be based on the assessment of specific biomarkers of the systemic response to impacts of shock waves of different frequency ranges. However, currently there is only limited information on early post-exposure changes in pro-inflammatory indices. The present study mostly focused on the temporal pattern of the systemic pro-inflammatory responses in an animal model of lung blunt trauma produced by exposure to low-frequency (260±5 Hz), long duration (~4 ms) shock wave with peak overpressure of 122 ± 8 kPa. The shock wave with these characteristics produced "moderate" lung injury that resulted in a consistent inflammatory response during the 24 h post-exposure period. In particular, we assessed the dynamics of PMN counts, surface expression of the CD11b adhesion molecule, and sequestration of [Fe^{3+}]TRF, the major carrier of blood plasma iron, in peripheral blood during post-trauma alterations.

We observed that the "moderate" lung injury from exposure to shock wave was accompanied by an increase in the number of circulatory PMNs as early as 1 h after BOP-exposure, which is indicative of mobilization of the pool of marginated PMNs into the free circulation, as has been postulated recently [25]. A further increase in PMN counts observed at 3 h post-exposure period was probably due to the rapid release of mature PMNs from bone marrow reserve [25]. Mobilization of large numbers of PMNs into the circulation enables the injured host to shuttle the granulocytes to injured tissues, where they mediate the healing process. Indeed, in our experiments infiltration of PMNs in hemorrhagic edema areas occurred as early as 3 h post injury and continued though the following 24 h. In the same time sequence as the PMN infiltration occurred the increase in the immunofluorescence of myeloperoxidase (a marker of PMN degranulation) was detected in alveolar septa of injured lung. After the increase in the number of circulatory PMNs at 1 h and 3 h, the numbers of circulatory PMNs began to decline at 6 h presumably due to tissue sequestration [25]. This is consistent with the pronounced induction of CD11b expression observed at the 3 h post-exposure period, which continued thoughout the twenty-four hour observation period. The expression of CD11b adhesion molecules on PMNs is an essential attribute specific for PMN interaction with the vascular endothelium [25].

It has been suggested that CD11b surface expression on PMNs is driven by pro-inflammatory cytokines (e.g. MIP-2 in rodents) and occurs before the PMNs reach the site of injury [25]. Our observation that MIP-2 levels increased 11-fold at 1 h post exposure to SW is consistent with that hypothesis, and suggests that MIP-2 plays a role in the increased expression of CD11b in circulatory PMNs prior to their migration into the lungs.

The systemic response to SW- induced trauma was associated with a decay in blood [Fe^{3+}]TRF complexes, as determined by EPR spectroscopy. TRF is the major carrier of [Fe^{3+}] in the extracellular blood liquid, and [Fe^{3+}]TRF can be detected in whole blood as well as in blood plasma, or serum. The TRF molecule containing two iron-binding sites in the C- and N-terminals can exist in both blood plasma and buffered solutions in four forms, iron-free or apo-, monoferric (C-terminal iron), monoferric (N-terminal iron), and diferric. At normal extracellular [Fe3+] concentrations random distribution of [Fe3+] on available TRF binding sites usually gives rise to a population of molecules of which ~50% are apo-TRF, ~40% monoferric, and ~10% diferric TRF [29].

EPR spectroscopy, like all other forms of spectroscopy, monitors the net absorption of energy from a radiation field when molecules change their energy state. The main feature of EPR spectroscopy is that it deals primarily with resonance microwave energy absorption by electron magnetic dipoles (spins) of paramagnetic centers (i.e. free radicals, metal ions) that is usually recorded as first derivative of absorption spectrum. [Fe^{3+}] ions distributed among the different [Fe^{3+}]TRF complexes have indistinguishable EPR parameters and, therefore, contribute equally to the low temperature EPR signals detected in solutions and biological samples. The EPR absorption of [Fe^{3+}]TRF complexes is proportional to the amount of the loaded iron, and the contribution of C- and N-monoferric, and diferric TRF to the EPR absorbance is additive, based on the amount of the chelated [Fe3+].

As follows from our results, at 24 h postexposure, the decrease in the level of blood plasma [Fe^{3+}]TRF correlated with injury levels. The observed tissue sequestration of [Fe^{3+}]TRF from blood was most likely essential for appropriate immune and/or hematopoietic responses to occur following damage [30, 31]. It is well documented that a fall in plasma iron concentration and alteration in the tissue distribution of iron are essential parts of the trauma-associated systemic response. In particular, acute conditions such as infectious diseases, myocardial infarction, fractures, wounds, and surgery are characterized by a profound and prolonged iron sequestration that lasts beyond the recuperation period. The mechanism of these phenomena remains unknown, however, it is considered to be a part of the acute phase non-immune inflammatory response which leads to turnover of iron though the TRF transport system.

In conclusion, the characteristics of a useful biomarker should include biomedical plausibility, sensitivity, specificity, reproducibility, ease of performance and low cost. One of the most important requirements is that the biomarker efficiently and effectively provides information pertained to the question being asked. The data presented suggest that assessment of [Fe^{3+}]TRF in blunt trauma can provide a good deal of information on severity of injury and satisfy most of the above requirements for an effective biomarker.

5.0 ACKNOWLEGMENTS

The views, opinions, and/or findings contained herein are those of the authors and should not be construed as an official Department of the Army position, policy, or decision, unless so designated by other documentation. We would like to express our gratitude to Ms. Jennifer Morris for her help in operation of the shock tube, and Dr Jayasree Nath for helpful suggestions and discussions during preparation of the presented data.

6.0 REFERENCES

[1] Hull JB, Cooper GJ: Pattern and mechanism of traumatic amputation by explosive blast. *J Trauma* 1996; 40(Suppl. 3): S198-S205.

[2] Coupland RM, Meddings DR. Mortality associated with use of weapons in armed conflicts, wartime atrocities, and civilian mass shootings: literature review. *BMJ* 1999; 319: 407-410.

[3] Cooper GJ. Protection of the lung from blast overpressure by thoracic stress wave decouplers. *J Trauma* 1996; 40 (Suppl. 3): S105-S110.

[4] Guy RJ, Glover MA, and Cripps NPJ. The pathophysiology of primary blast injury and its implications for treatment. *J R Nav Med Serv* 1998; 84:79-86.

[5] Sturdivan LM, Viano DC, Champion H. Analysis of injury criteria to assess chest and abdominal injury risks in blunt and ballistic impacts. *J Trauma* 2004; 56:651-663.

[6] Stumiller JH. Biological response to blast overpressure: A summary of modeling. *Toxicology* 1997; 121: 91-103.

[7] Harmon, JW, Sampson JA, Graeber GM, et al. Readily available serum chemical markers fail to aid in diagnosis of blast injury. *J Trauma* 1988; 28 (Suppl.1): S153- S159.

[8] Dedushkin VS, Kosachev ID, Tkachenko SS, et al. Rendering medical care and the volume of the treatment of victims with blast injuries. *Voen Med Zh* 1992; 1: 13-18.

[9] Cernak I, Savic J, Zunic G, et al. Recognizing scoring, and predicting blast injuries. *World J Surg* 1999; 23: 44-53.

[10] Cooper GJ, Townend DJ, and Cater SR. The role of stress waves in thoracic visceral injury. *J Biomech* 1991; 24: 273-285.

[11] Chen H, Wang Z, Ning X, Xu H, Xiao K. Animal study on lung injury caused by simulant segmented shock waves. *Chin J Traumatol* 2001; 4:37-39.

[12] Bowen IG, Fletcher ER, Richmond DR, et al. Biophysical mechanisms and scaling procedures applicable in assessing responses of the thorax energized by air-blast overpressores or by nonpenetrating missiles. *Ann NY Acad Sci* 1968; 152: 122-146.

[13] Guy RJ, Watkins PE, and Sdmondstone WM. Electrocardiographic changes following primary blast injury to the thorax. *J R Nav Med Serv* 2000; 86:125-133.

[14] Guy RJ, Kirkman E, Watkins PE, et al. Physiologic responses to primary blast. *J Trauma* 1998; 45: 983-996.

[15] Maynard RL, Cooper GL, and Scott R. Mechanism of injury in bomb blasts and explosions. In: Westaby S (Ed). *Trauma – Pathogenesis and Treatment* London. Heinemann. 1988, pp. 30-41.

[16] Kushner I. The phenomenon of the acute phase response. *Ann NY Acad Sci* 1982; 389: 39-48.

[17] Yang F, Liu X, Quinones M, et al. Regulation of reticuloendothealial iron transporter MTP1 (Slc11a3) by inflammation. *J Biol Chem* 2002; 277: 39786-39791.

[18] Hirose M. The structural mechanism for iron uptake and release by transferrins. *Biosci Biotechnol Biochem* 2000; 64: 1328-1336.

[19] Walsh DS, Pattanapanyasat K, Lamchiagdhase P, et al. Iron status following trauma, excluding burns. *Br J Surg* 1996; 83: 982-985.

[20] Gorbunov NV, Nath J, Parker JM, et al. Electron paramagnetic resonance analysis of transferrin-bound iron in animal models of blunt trauma. *J Trauma* 2003; 54: 574-583.

[21] Yelverton JT: Pathology scoring system for blast injuries. *J Trauma* 1996; 40 (Suppl. 3): S111-S115.

[22] Elsayed NM. Toxicology of blast overpressure. *Toxicology* 1997; 121: 1-15.

[23] Gorbunov NV, Pogue-Geile KL, Epperly MW, et al. Activation of the nitric oxide synthase 2 pathway in the response of bone marrow stromal cells to high doses of ionizing radiation. *Radiat Res* 2000; 154: 73-86.

[24] Abraham E, Carmondy A, Shenkar R, et al. Neutrophils as early immunologic effectors in hemorrhage- or endotoxemia-induced acute lung injury. *Am J Physiol Lung Cell Mol Physiol* 2000; 279: L1137-L1145.

[25] Botha AJ, Moor FA, Moor EE, et al. Early neutrophil sequestration after injury: a pathogenic mechanism for multiple organ failure. *J Trauma* 1995; 39: 411-417.

[26] Maynard RL, Cooper GL, Scott R: Mechanism of injury in bomb blasts and explosions. In: Westaby S (Ed). *Trauma – Pathogenesis and Treatment* London. Heinemann. 1988; pp. 30-41.

[27] Bowler RP, Arcaroli J, Crapo JD, et al. Extracellular superoxide dismutase attenuates lung injury after hemorrhage. *Am J Respir Crit Care Med* 2001; 164:290-294.

[28] Cooper GJ, Maynard RL, Cross NL, et al. Casualties from terrorist bombings. *J Trauma* 1983; 23: 955-967.

[29] Young SP, Bomford A, Williams R. The effect of the iron saturation of transferrin on its binding and uptake by rabbit reticulocytes. *Biochem J* 1984; 219: 505-510.

[30] Laterveer L, Lindley IJD, Hamilton MS, et al. Interleukin-8 induces rapid mobilization of hematopoietic stem cells with radioprotective capacity and long-term myelolymphoid repopulating ability. *Blood* 1995; 85: 2269-2275.

[31] Wang J, Zhang Y, Kasahara T, et al. Detection of mouse IL-8 receptor homologue expression on peripheral blood leukocytes and mature myeloid lineage cell in bone marrow. *J Leukoc Biol* 1996; 60: 372-381.